

Stark-Cyclotron Resonance in a Semiconductor Superlattice

Luca Canali,¹ Marco Lazzarino,² Lucia Sorba,^{2,*} and Fabio Beltram^{1,2}

¹*Scuola Normale Superiore and Istituto Nazionale per la Fisica della Materia, I-56126 Pisa, Italy*

²*Laboratorio TASC dell'Istituto Nazionale per la Fisica della Materia, I-34012 Trieste, Italy*

(Received 13 October 1995)

Electron transport in crystals in intense parallel electric and magnetic fields is investigated. Current resonances are shown for particular ratios of electric and magnetic fields satisfying the Stark-cyclotron resonance (SCR) condition. At SCR, the potential drop per period is an integer multiple of the magnetic quantization energy and elastic tunneling transport between Landau levels belonging to neighboring crystal sites becomes possible. Unambiguous demonstration of SCR in an appropriately tailored heterojunction superlattice is given for transitions involving up to four Landau-level index changes. [S0031-9007(96)00176-7]

PACS numbers: 72.20.My, 76.40.+b, 73.50.Jt

After the birth of quantum mechanics electron transport studies in crystals acquired a new meaning and importance. In fact, they have proved very effective tools to probe electronic states and energy levels in solids. We report here on the manifestation in transport of spectrum discretization and the localization of corresponding states occurring when intense electric and magnetic fields are superimposed on a periodic potential. This quantum mechanical behavior is demonstrated for the first time by the observation of particular current resonances.

In the absence of perturbations to the periodic crystal potential, electronic states are delocalized over the entire solid and the energy spectrum consists of allowed energy bands separated by forbidden *gaps*. Wannier [1] showed that an external electric field localizes electronic states along the field direction into the now-called Wannier-Stark states, whose extension is inversely proportional to the applied field. Correspondingly, the energy spectrum is drastically modified: Each band breaks down into a *Wannier-Stark ladder*, a set of subbands separated in energy by eFd , where e is the electronic charge, F the applied electric field, and d the period of the crystal (we assume a one-dimensional structure for simplicity). The experimental confirmation of this picture was achieved only relatively recently and was made possible by the introduction of the concept of heterojunction superlattice (SL) by Esaki and Tsu [2].

A SL is an artificial crystal constituted by a periodic arrangement of thin films of different semiconductors. A steplike effective potential in the growth direction is generally used to model electronic dynamics in these structures [3]. The discontinuities in the effective potential are linked to the different gaps of the constituents and identify *well* and *barrier* layers (see Fig. 1, where the conduction band of a SL is sketched in the bias conditions here of interest). Crystal parameters can be tailored over a wide range of values changing semiconductor types and/or well and barrier thicknesses. In particular, Wannier-Stark localization is made accessible to experimental demonstration in SLs

and was demonstrated in these crystals by optical [4] and transport measurements [5].

Wannier-Stark levels cannot be resolved when their broadening (Γ) is greater than their energy separation, i.e., when $\Gamma > eFd$. By this argument a critical field F_c can be introduced such that $eF_c d = \Gamma$. For $F < F_c$ current increases with applied electric field (reducing to Ohm's law for $F \ll F_c$), while in the case $F > F_c$ current proceeds by hopping between neighboring Wannier-Stark states. Their increasing localization with F leads to current decreasing with applied field. This gives rise to negative differential conductance (NDC) in the current-voltage (I - V) characteristic [2,6]. In "natural" crystals this phenomenon was never observed since F_c is of the same order of magnitude as the threshold field for Zener (interband) tunneling, which overwhelms the NDC signal.

Upon application of high electric and magnetic fields parallel to the SL growth axis, assuming parabolic disper-

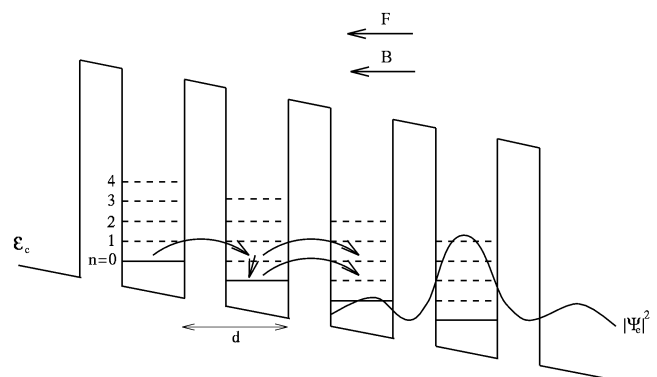


FIG. 1. Schematic conduction-band profile (E_c) of a superlattice in parallel electric (F) and magnetic (B) fields. Bias conditions illustrate Stark-cyclotron resonance ($eFd = \delta n \hbar \omega_c$, where ω_c is the cyclotron frequency) for the case of Landau-level index change $\delta n = 1$. Wannier-Stark-Landau levels are represented for n up to 4. Some possible transport paths are indicated by arrows together with the sketch of a Wannier-Stark state (ψ_e).

sion the energy spectrum is given by [7]

$$E_{\nu,n} = (eFd)\nu + \hbar\omega_c(n + \frac{1}{2}), \quad (1)$$

where $\nu = 0, \pm 1, \pm 2, \dots$ is the Wannier-Stark index, $\omega_c = eB/m^*$ is the cyclotron frequency, B is the magnetic field, m^* is the effective mass, and $n = 0, 1, 2, \dots$ is the Landau index. This modified spectrum was experimentally analyzed by the optical measurements of Alexandrou, Mandez, and Hong [8]. Corresponding states will be called Wannier-Stark-Landau (WSL) states. We shall factorize WSL states by decoupling the motion along the growth axis and in the plane of the layers. Along the growth axis WSL states are localized Wannier states, as previously discussed. In the layer planes when $B = 0$ electronic states are plane waves, while in the presence of nonzero magnetic field they are Landau states [9]. The discrete nature of the spectrum is a direct consequence of this further localization.

In this Letter we study electronic transport in the presence of intense parallel electric and magnetic fields. We shall present the first experimental demonstration of elastic transport resonances that stem from the interplay between electric and magnetic fields in a GaAs/Al_{0.3}Ga_{0.7}As SL grown by molecular beam epitaxy (MBE).

When both fields are present current proceeds mainly by inelastic hopping between WSL states belonging to neighboring wells [10,11]. Here we want to focus, in particular, on the situation when WSL states with different Landau (n) and Wannier-Stark (ν) indices are isoenergetic. This is called the Stark-cyclotron resonance (SCR) condition. It is important to note that at resonance coherent tunneling between WSL levels with different Landau indices is forbidden by the Landau-index selection rule, while tunneling assisted by elastic scattering is allowed [12,13]. The analytical expression of SCR is

$$eFd = \delta n \hbar\omega_c, \quad (2)$$

where δn is an integer number representing the Landau-level index change and is illustrated in Fig. 1 for the case $\delta n = 1$. Electronic transport in this situation was investigated theoretically by several authors, considering the effects of the angle between electric and magnetic fields [14], acoustic-phonon-assisted quasielastic scattering [13], and impurities [12]. Whenever the SCR condition is met, current is expected to increase owing to the onset of the new elastic transport channel. The resulting current peaks are the manifestation in the transport of SCR.

An important check must be performed in order to establish the observability of these resonances. Scattering times have been estimated by Ferreira [12] for a GaAs/AlGaAs SL with an impurity layer concentration of 10^{10} cm^{-2} . Ferreira showed that elastic and inelastic times can be of the same order of magnitude and predicted SCR oscillations for the elastic component of the current [12]. Another factor favoring the observation of SCR in transport is the suppression of inelastic scattering caused by a magnetic

field which produces a threshold for inter-Landau-level transitions involving phonon emission [15]. As shown in Fig. 1, after the elastic transition current can proceed by intrawell relaxation and further tunneling. Multiple scattering processes could also play a role (see Fig. 1).

In order to demonstrate SCR, a suitable heterostructure was designed and grown by MBE. Essential requirements are a sufficiently large miniband dispersion in order to ensure SL formation and a wide minigap to suppress interminiband tunneling in the bias region of interest [5]. The SL studied is nominally undoped and consists of 14 periods of 50 Å thick GaAs well and 34 Å thick Al_{0.3}Ga_{0.7}As barrier. The ground-state miniband has a calculated dispersion of 23 meV and is separated from the first-excited one by a 130 meV wide minigap. SL growth was preceded by an injector structure composed of three thin (12 Å) barriers separated by wells 128, 81, and 81 Å thick, respectively. This structure was introduced to reduce the potential threshold for electron injection into the first miniband. The first barrier of the SL, on the injector side, was grown thicker (93 Å) to reduce current injection into the structure and consequently improve electric-field homogeneity in the SL region. After the SL a nominally undoped 0.2 μm thick GaAs layer was grown. These layers are enclosed between two 0.5 μm thick Si-doped $n \approx 10^{18} \text{ cm}^{-3}$ GaAs layers. The structure was fabricated by standard photolithographic and wet-etching techniques. Individual devices are 75 μm diameter circular mesas to which contacts were provided. I - V measurements were performed with a HP4142B. Magnetic fields up to 9.2 T were produced by a NbTi superconducting magnet. Temperature was varied in a closed-cycle ³He refrigerator in the 0.3–200 K range.

Figure 2 shows the I - V characteristic at 4.2 K and zero magnetic field, positive biases refer to electron injection

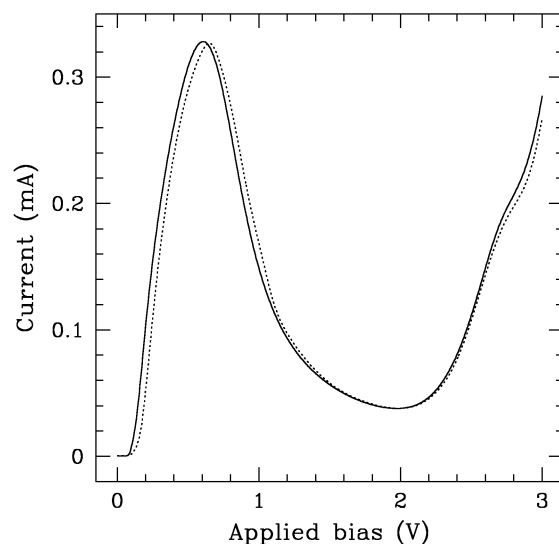


FIG. 2. Current vs voltage characteristic at 4.2 K in the absence of magnetic field (solid line) and at 8 T (dotted line).

from the injector side. Typical miniband transport behavior can be seen. At low fields current monotonically increases, while at higher fields NDC is observed. No space charge effects are present in our structure. In fact, by taking into account the carrier velocity in the miniband regime and the current density, one obtains an upper limit for the carrier density $\sim 10^{13} \text{ cm}^{-3}$ [16]. For biases higher than about 1.5 V tunneling current into the first excited miniband becomes observable. From about 2.0 V it dominates the I - V and NDC is suppressed. In this region at $V_{\text{bias}} \approx 2.6 \text{ V}$, a shoulder can be observed. As will be apparent from the data of Table I, this bias corresponds to a potential drop per period of about 77 mV: It can be inferred that this shoulder is due to sequential resonant tunneling [16] into the excited subband of the second neighbor well (at flat bands the calculated energy separation between levels is 160 meV). Here we are interested in the NDC region where current proceeds mainly by hopping between Wannier-Stark levels (bias range 0.6–1.5 V).

Setting the bias and consequently the electric field in the SL by varying the applied magnetic field SCR will manifest as current peaks. Indeed we found resonances in current vs magnetic field (I - B) characteristics with applied biases in the NDC region as reported in Fig. 3 for three values $V_{\text{bias}} = 0.84, 1.02, \text{ and } 1.22 \text{ V}$ [17]. These peaks occur on an increasing background due to the semiconductor bulk positive magnetoresistance. This behavior is linked to the negative slope of the I - V at the biases of Fig. 3 (see also Fig. 2). The amplitude of SCR peaks is of the order of 1% indicating that inelastic hopping is the dominant transport mechanism. Peaks occurring at higher magnetic fields are noticeably more pronounced in agreement with the arguments of Ref. [15]. To relate the experimental resonances to SCR, magnetic-field peak positions (B_p) were extracted from the I - B characteristics for different biases (V_p) within the bias range of the NDC region.

In Fig. 4 (B_p, V_p) points are plotted in an applied magnetic field vs bias (B - V) plane. Experimental points clearly align along four straight lines, in agreement with (2). In order to model the observed peak positions one must consider that at equilibrium the SL is subject to a built-in electric field so that flat-band conditions in the SL are reached upon application of an external bias $V_0 \approx$

TABLE I. Linear least square fit $B_p = a(V_p - V_0)$ for the data of Fig. 4 ($V_0 = 0.2 \text{ V}$, see text). Resonances are labeled by the Landau-level index change (δn) identified by computing the ratios $a(1)/a(\delta n)$.

Resonance	a	
δn	(T/V)	$a(1)/a(\delta n)$
1	21.3 ± 0.5	...
2	11.9 ± 0.1	$a(1)/a(2) = 1.8 \pm 0.1$
3	7.0 ± 0.1	$a(1)/a(3) = 3.0 \pm 0.2$
4	5.1 ± 0.1	$a(1)/a(4) = 4.2 \pm 0.2$

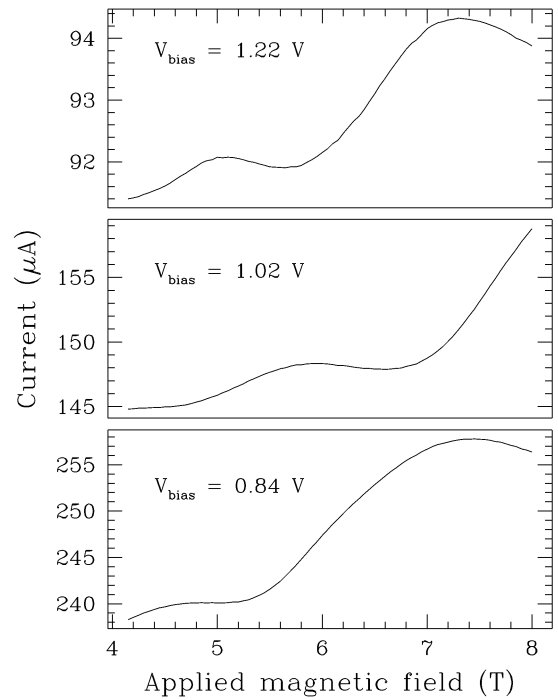


FIG. 3. Current vs magnetic-field characteristics for three different bias conditions, $V_{\text{bias}} = 0.84 \text{ V}$ (lower panel), $V_{\text{bias}} = 1.02 \text{ V}$ (middle panel), and $V_{\text{bias}} = 1.22 \text{ V}$ (upper panel). Measurements were performed at 4.2 K.

0.2 V [18]. For this reason and the above mentioned field homogeneity, electric field in the SL can be given by $F \propto (V - V_0)$. By these arguments the SCR condition can be expressed by $B_p \propto (V_p - V_0)/\delta n$. Note, in particular, that the slope is inversely proportional to the Landau-level index change δn . We report in Table I the values of the fitted slopes for the four lines considered. By computing the ratios of the slopes over that of the left-most line,

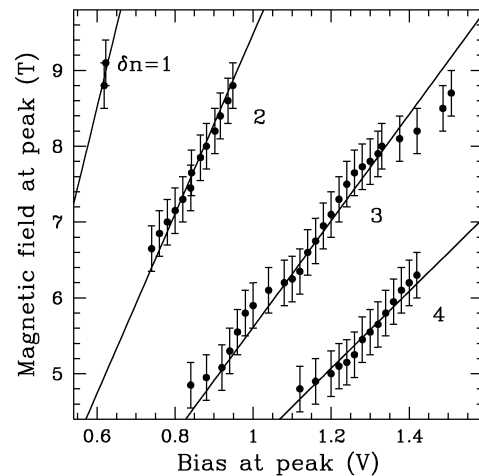


FIG. 4. Experimental magnetic field and applied bias at Stark-cyclotron resonance (SCR). Also shown are the fits with parameters defined in Table I. δn is defined by the SCR condition $eFd = \delta n \hbar \omega_c$ and is derived from the data of Table I.

agreement is found with the SCR condition and transitions with $\delta n = 1, 2, 3,$ and 4 are unambiguously identified.

SCR is observable only in a region of the B - V plane experimentally defined by $0.6 \leq V_p \leq 1.5$ V and $B_p \geq 5$ T. An additional limitation stems from the highest magnetic field available (9.2 T in our case). In fact, for lower biases Wannier-Stark levels are not resolved because of broadening, while for larger electric fields current is dominated by tunneling into the excited miniband. For low magnetic-field intensities, in turn, Landau levels are not resolved because of broadening. Finally, note that SCR transitions with $\delta n \geq 5$ are not observable in the present sample because they lie in the forbidden low magnetic-field and interminiband tunneling regions.

The broadening Γ can be estimated independently from $\Gamma = eF_c d$ and $\Gamma = \hbar e B_t / m^*$, where F_c is the critical field for NDC and B_t is the threshold magnetic field. Both expressions are consistent with $\Gamma \sim 10$ meV, a value ascribable mainly to inhomogeneous broadening [16].

As mentioned above several scattering mechanisms can contribute to make SCR observable in transport. By analyzing the temperature dependence of the I - B characteristics we have not observed any significant change in the characteristics in the 0.3–50 K range. This indicates that acoustic-phonon-assisted (quasielastic) transport is not dominant. The SL is nominally undoped but we can estimate a p -type (carbon) background residual doping of the order of 10^{15} cm $^{-3}$. Elastic scattering with ionized background impurities [12] and with layer fluctuations are the main mechanisms assisting resonant transport in the low-temperature range. At temperatures above 50 K the NDC region (and consequently SCR signal) is increasingly suppressed by the rising thermally assisted tunneling current.

In conclusion, we have reported the first observation of the Stark-cyclotron resonance, a quantum mechanical effect caused by the localization of electronic states in crystals produced by intense parallel electric and magnetic fields. This leads to singularities in the density of states that have been proved in high-field magnetotransport experiment on an artificially tailored crystal synthesized by epitaxial technique.

The authors gratefully acknowledge F. Capasso and R. A. Suris for stimulating discussions.

*Also with CNR-ICMAT, Montelibretti, Roma, Italy.

- [1] G.H. Wannier, *Elements of Solid State Theory* (Cambridge University Press, London, 1959), pp. 190–193.
- [2] L. Esaki and R. Tsu, IBM J. Res. Dev. **14**, 61 (1970).
- [3] See, e.g., G. Bastard, *Wave Mechanics Applied to Semiconductor Heterostructures* (Halsted Press, New York, 1988).
- [4] E. E. Mendez, F. Agulló-Rueda, and J.M. Hong, Phys. Rev. Lett. **60**, 2426 (1988).
- [5] F. Beltram, F. Capasso, D.L. Sivco, A.L. Hutchinson, S.G. Chu, and A.Y. Cho, Phys. Rev. Lett. **64**, 3167 (1990).
- [6] B. S. Shchamkhalova and R.A. Suris, Superlattices Microstruct. **17**, 151 (1995).
- [7] F. Claro, M. Pacheco, and Z. Barticevic, Phys. Rev. Lett. **64**, 3058 (1990).
- [8] A. Alexandrou, E. E. Mendez, and J. M. Hong, Phys. Rev. B **44**, 1934 (1991).
- [9] See, e.g., L.D. Landau and E.M. Lifshitz, *Quantum Mechanics Non Relativistic Theory* (Pergamon Press, Oxford, 1965).
- [10] V. V. Bryksin and Yu. A. Firsov, Fiz. Tverd. Tela (Leningrad) **15**, 3235 (1973) [Sov. Phys. Solid State **15**, 2158 (1974)].
- [11] Y. Lyanda-Geller and J-P. Leburton, Phys. Rev. B **52**, 2779 (1995).
- [12] R. Ferreira, Phys. Rev. B **43**, 9336 (1991).
- [13] V.M. Polyakovskii, Fiz. Tekh. Poluprovodn. **15**, 2051 (1981) [Sov. Phys. Semicond. **15**, 1190 (1981)].
- [14] F.G. Bass, V.V. Zorchenko, and V.I. Shashora, Pis'ma Zh. Eksp. Teor. Fiz. **31**, 345 (1980) [JETP Lett. **31**, 314 (1980)]; F.G. Bass and V.M. Polyakovskii, Fiz. Tekh. Poluprovodn. **21**, 1207 (1987) [Sov. Phys. Semicond. **21**, 733 (1987)].
- [15] A. Kastalsky and A.L. Efros, J. Appl. Phys. **69**, 841 (1991).
- [16] F. Capasso, K. Mohammed, and A. Y. Cho, IEEE J. Quantum Electron. **22**, 1853 (1986).
- [17] SCR peaks are present also in I - V characteristics at constant applied magnetic field, but since they occur on a rapidly varying background they are less easily identifiable, particularly at lower magnetic fields (see also Fig. 2 where the I - V in the presence of $B = 8$ T is shown).
- [18] This field stems from band bending in the nominally undoped region at equilibrium.